An Experimental Investigation of the Changes of VLBI Time Delays Due to Antenna Structural Deformations

T. Y. Otoshi
Radio Frequency and Microwave Subsystems Section

L. E. Young
Tracking Systems and Applications Section

An experimental investigation was conducted on the 64-m antenna at DSS 14 to study the effects of antenna structural deformations on VLBI time delays at S-band. Structural deformations primarily occur as functions of antenna elevation angle due to gravity loading. For a Cassegrain antenna, one of the major effects of structural deformation on measured VLBI time delays are those delay changes associated with axial subreflector displacement from its nominal position. Two types of time delay changes that occur when the subreflector is axially defocused are (1) a change which is a linear function of subreflector defocus position and (2) a cyclical change caused by multipath. Test results showed that for the 64-m DSN antenna, the linear change is 1.8 times the subreflector defocus position, while the peak-to-peak change in cyclical variation is about ±3 cm when a spanned bandwidth of 38 MHz at 2290 MHz is used.

I. Introduction

When a large antenna is used to track a signal coming from a spacecraft or VLBI radio source, gravity loading causes deformations of the antenna structure as functions of antenna pointing angles. If the resulting changes in antenna time delays are not properly taken into account, significant errors could occur in the determination of spacecraft position, station location, or other uses of VLBI data such as for studies of earth crustal movements.

It was shown in a structural deformation study by Katow (Ref. 1) that when the antenna points at elevation angles different from optimum 45 deg, structural deformation of the antenna will occur due to gravity loading. Four structural deformation variables that affect time delay changes were shown to be displacements of the best-fit paraboloid focal point, paraboloid vertex, feed horn phase center, and subreflector vertex. The displacements were analyzed as functions of elevation angle relative to the optimum 45-deg elevation angle parameters which in turn are referenced back to the station location (intersection of Az-El axes). Of the various displacements mentioned, defocusing (and refocusing) of the subreflector was shown to contribute the largest changes in VLBI time delays as functions of elevation angles.

On August 23, 1980, VLBI experiments were performed on the 64-m antenna at DSS 14 (Fig. 1) for purposes of simulating gravity loading and measuring associated time delay changes. One of the simulation experiments performed was to isolate and measure the time delay changes associated with axial subreflector defocusing. This article will describe the experimental procedure and also the data processing methods involved in obtaining the 1- to 2-cm accuracy required to observe the multipath effects when using VLBI bandwidth synthesis (BWS) channel separations of about 40 MHz. The experiment described in this article is believed to be the first use of VLBI data taken specifically for comparison to antenna multipathing theory.

II. Discussion of the Antenna Multipath Phenomenon

Figure 2 shows the geometry of the DSS 14 Cassegrain antenna with a reflex-dichroic system which enables simultaneous receptions of both S- and X-band frequencies. A signal originating from the far field is collected by the parabolic reflector, reflected to the subreflector, re-reflected, and arrives at the receive horn via the ray paths of the dual-band system. If the antenna is ideal, all signals follow geometric optics (GO) ray paths so that they all have the same delay (path length) from the paraboloid focal plane to the system feed horn focal point. In practice numerous factors such as blockage, mechanical supports, imperfect reflector surfaces, mechanical distortions, and defocusing cause departure from the ideal Cassegrain antenna. Furthermore, two known types of multipath signals are generated within the antenna optics medium of practical Cassegrain antennas. The first type is caused by a portion of the illuminating plane wave signal becoming blocked by the large subreflector and subreflector support struts. Diffraction around the edges of the subreflector and struts will occur and a portion of these diffracted fields propagates directly into the receive horn. Another type of multipath phenomenon that occurs is that generated by unwanted multiple reflections between the subreflector and feedcone surfaces as illustrated in Fig. 3.

When the subreflector of a Cassegrain antenna defocuses in the axial direction, two types of VLBI time delay changes occur, namely: (1) a linear time delay change due to geometric path length changes related to the subreflector displacement and (2) a cyclical time delay change due to multiple reflection multipath signals of the type depicted in Fig. 3. Both types of changes were previously analyzed theoretically through the use of electromagnetic theory principles and antenna computer programs developed specifically to study the effects of defocusing and multiple reflections between the subreflector and feedcone support surfaces (Ref. 2). A typical theoretical curve showing the linear and cyclical variation is depicted in Fig. 4.

If one desires a quick estimate of the effects of subreflector defocusing, the following approximate formula can be used to compute the delay change in nanoseconds.

$$\Delta\tau_{BWS} = \frac{K_1 \Delta S}{c} + \frac{A}{\pi \Delta f} \sin\left[\frac{\pi \Delta f x}{c}\right] \cos\left[\frac{2\pi f_0 x}{c} - \psi\right] \tag{1}$$

where

$$x = \ell_2 - \ell_1 \cong 2d + (K_2 - K_1)\,\Delta S \tag{2}$$

and

K_1, K_2 = constants relating pathlength changes to subreflector movement for the primary and secondary signals, respectively, and are approximately equal to 1.8 and 3.8, respectively.

ΔS = subreflector defocus position relative to the nominal position, cm

c = speed of light (29.97925 cm/ns)

A = voltage ratio of the multipath signal to the primary signal

Δf = spanned bandwidth = $(f_B - f_A)$

f_0 = center frequency = $(f_B + f_A)/2$

f_B = upper frequency used in VLBI BWS measurement, GHz

f_A = lower frequency used in the VLBI BWS measurement, GHz

ℓ_1, ℓ_2 = path lengths of the primary and secondary signals, respectively, cm

d = nominal distance between the subreflector vertex and cone platform surface creating the multipath signal, cm

ψ = phase angle which establishes where the multipath cyclical pattern begins, radians

Equation (1) was derived by first taking the phase term given in Ref. 3 and applying it to the BWS equation (Ref. 4) at the two channel frequencies involved in the BWS measurements. Then assuming that the multipath signal is small, i.e. $A < 0.1$ and using trigonometric identities, the approximate formula given by Eq. (1) was obtained.

The approximate formula given above will yield a theoretical multipath amplitude ripple that is slightly larger than those obtained from the Rusch Computer Program (Ref. 2). Since this approximate formula does not account for edge diffractions, it does not give sufficient damping of the sinusoidal features. However, the approximate formula can be very useful for obtaining quick estimates of error bounds and for making quick comparisons to experimental subreflector defocus data. The formula is also useful for clearly showing that multipath error (the cyclical term) decreases as spanned bandwidth is increased.

III. Description of Experiment

One of the major experiments performed on the 64-m antenna at DSS 14 was to isolate and measure the time delay changes associated with axial subreflector defocusing. The experiment consisted of observing a radio source simultaneously with the 26-m antenna at DSS 13 and the 64-m antenna at DSS 14. The signal outputs from three 1.8-MHz-wide channels were recorded on magnetic tape at each station. Hydrogen masers provided the basic frequency standards at each station and provided the clock (timing) signals. At each station, phase calibration signals were injected into the incoming signal stream at an injection port close to the output of the feed horn assembly. As discussed in Ref. 4, the phase calibration signals are used to remove instrumental delay changes that occur below the injection port at each station. Removal of these instrumental delays enables the isolation and measurement of only those delay changes caused by antenna optics structural deformations and changes in the transmission media above the antenna. Since the DSS 13-14 baseline is short (21.6 km), the assumption is made that the transmission media (consisting of troposphere, ionosphere, and plasma) are similar above the two stations. Any delay changes in this transmission media during the experiment should cancel out in the VLBI correlation processing because of common-mode rejection. The shortness of the baseline also affords the additional advantages of reduced sensitivity to errors in source position, universal time, and polar motion.

The experiment was performed with a 2290-MHz center frequency and at various spanned bandwidths (SBW), with the largest SBW being 38 MHz. The 26-m antenna at DSS 13 was used as the reference antenna, with its subreflector fixed in the nominal position throughout the test. Only the subreflector on the 64-m antenna was defocused. For this experiment to be valid, the DSS 13 antenna delay must not vary radically with antenna pointing angles. An X-band test performed by Freily (Ref. 6) showed that the DSS 13 antenna gain changes were small as functions of elevation angle. If the reported small gain changes for this antenna were due primarily to structural deformations, it is reasonable to expect that phase and group delay changes for the DSS 13 antenna would also be small. If slowly varying group delay changes do occur on the DSS 13 antenna, most of the effects of this drift are later removed by polynomial curve fits performed on repeated points taken under nominal conditions.

The VLBI experiments for the results of this article were specifically designed to enable accurate measurements of multipath-caused delay changes as functions of axial subreflector defocusing. First, in order to minimize the delay changes contributed by the ionosphere and temperature variations, the experiments were purposely scheduled to be performed during local nighttime hours. Secondly, a radio source was selected on the basis that it would (1) provide adequate signal-to-noise ratio, (2) be essentially unresolved (unstructured) over the DSS 13 – DSS 14 baseline and (3) remain at nearly constant elevation angles in the region of 45 to 60 deg throughout the major portion of test times. It was desirable that the antenna be pointed at nearly constant elevation angles so that gravity loading would be constant and not cause unknown or unwanted subreflector movements.

A factor which must be considered in an experiment of this type is the wind velocity and its direction relative to the paraboloid reflector surface. It was fortunate that for this particular experiment the wind velocity was less than 9.7 kph (6 mph) throughout the test period. Using the wind study results reported by R. Levy (Ref. 5), it could be concluded that only negligible errors could be contributed to this experiment by 9.7-kph wind loading or wind gusts.

The experimental procedure for the axial subreflector test was to move the subreflector sequentially from a positive defocus position on one side of nominal setting, then to a negative defocus position (of nearly equal increment) on the other side of nominal setting, and then back to nominal setting. At each of these subreflector positions, a measurement was made for a period of about 2 minutes duration. All data were purposely taken in this manner relative to the nominal setting so that polynomial curve fits could later be performed on the nominal points to enable removal of long-term drifts (such as those due to clock frequency offsets, antenna elevation angle dependence, geometric delay modeling errors, etc.). The total range of defocus of the subreflector from its nominal position for this test was plus/minus 6 cm. Three separate runs were made using the above described test procedure.

Postprocessing of the data consisted of the following five steps:

(1) Performing a correlation of the data recorded on magnetic tapes through the use of the Caltech/JPL Block 0 VLBI correlator giving the total time delay of the DSS 13 – 14 baseline

(2) Applying phase calibrator corrections for each station to remove instrumental delay part of the total delay

(3) Using the VLBI Fit Delay Program to remove the geometric delays, long-term drifts, and residual clock errors so that the remaining delay changes could be attributed to changes occurring only in the antenna optics region

(4) Performing further data reduction necessary to express the results in terms of antenna test parameters

(5) Correlating the final processed data with antenna theory.

IV. Test Results

Figure 5 shows a plot of nominal point test data after correlations on the VLBI data recorded on magnetic tapes were performed. The purpose of showing this plot is to show the magnitude of long-term drift due to residual clock errors, and to show that most of this drift will be ultimately removed by the Fit Delay Program. An unweighted third-order polynomial curve was fitted to the points and shows that the drift is of the order of 140 cm over the test period of about 8 hours. Also indicated on the plot are the time periods of the axial subreflector test runs and the corresponding antenna elevation angles.

Figure 6 shows a plot of the scatter of the nominal points when the Fit Delay Program was used to perform a *weighted* polynomial curve fit routine on the nominal data points. The weights were based on error estimates derived directly from the outputs of the VLBI correlator. It should be mentioned that the residual errors shown in Fig. 6 were arrived at by judiciously dividing the total test time into three sections and performing separate fit delay second-order polynomial curve fits to the nominal points in each section. Division into three sections was necessary because the long-term drifts over 8 hours could not be accurately characterized by a single second-order polynomial. The deviations of the nominal points were computed by the Fit Delay Program to have an rms value of 1.5 cm, which is a useful value for estimating the type of accuracy that can be achieved by this experiment.

After deriving the best-fit curve to the nominal points, the Fit Delay Program then computes deviations of nonnominal points from the curve. These deviations are the test data of interest and are shown plotted in Fig. 7 for the three subreflector defocusing tests performed within the same 8-hour time span. These data have been corrected with phase calibration data for both DSS 13 and 14. The vertical scale is shown in units of equivalent freespace path length units, while the horizontal axis is the axial subreflector defocus position (relative to the nominal position).

Since it is known from theory (see Section II of this article) that the delay changes caused by axial subreflector defocusing will consist of a linear term and a cyclical term, it is desirable to perform a least squares fit using a theoretical model that contains both terms. However, it is difficult to perform a least squares fit using the more accurate theoretical model developed by Rusch (Ref. 2) because numerical solutions from his analysis are arrived at by an iterative process that cannot be expressed in closed form. A study is currently being made to perform a least squares fit using the approximate expression given in Eq. (1). The results of this work will be reported in a future TDA Progress Report.

The alternative data reduction approach that was used for the results of this article was to do the curve fitting in a sequential manner. First a linear fit was performed on the total data and then a multipath curve fit was made to the residuals. Although this alternate procedure is not as theoretically rigorous as curve fitting to both linear and cyclical terms simultaneously, it did enable results to be obtained in an expedient manner using available computer programs. A weighted linear curve was fitted to the test data from all three subreflector tests using weights based on error estimates of each test data point and the rms error of the nominal points shown in Fig. 6. Figure 7 shows the resulting linear curve together with its standard error limits as indicated by the edges of the shaded area. The standard error is a function of subreflector setting and is the largest (±0.4 cm) at the outer edges (±6.6 cm) of the plot. The slope of the best fit linear curve to experimental data is 1.77, which is in excellent agreement with the theoretical slope value of 1.76 reported in Ref. 2. This agreement is fortuitous because of the apparent cancellation of the multipathing signature.

It is important to emphasize that the slope of the linear curve is about 1.8 and not the 2.0 value most often used for crude estimates. The actual slope will generally be less than 2.0 and will be different for each Cassegrain antenna. The 2.0 slope applies only to a single ray on the paraboloid axis of symmetry, while the true slope is dependent upon the total primary feed amplitude pattern, the subreflector scattered patterns at the different defocus positions, and the corresponding changes in the amplitude and phase over the entire paraboloidal aperture. These dependent factors are all taken into account in the Rusch program (Ref. 2), when integrations are performed over the entire paraboloidal antenna aperture.

Figure 8 shows the residuals after the best fit linear curve was subtracted from the data points shown in Fig. 7. For purposes of comparison with antenna theory, a theoretical multipath curve was generated by the Rusch program for the multi-

path geometry on the 64-m antenna at 2290 MHz and 38 MHz SBW. The theoretical curve is shown as the dashed line and was "eye-ball" fitted by lining up the peak of the theoretical curve with the peak data points at about the negative 2-cm defocus position on the X-axis and centering the curve symmetrically about the Y-axis. The solid line theoretical curve shown in the same plot was generated from use of the second term of the approximate equation given in Eq. (1), assuming that the multipath signal was −36 dB (corresponding to $A = 0.016$) down from the primary signal. Other parameters used to generate this solid curve were $d = 1657$ cm, $K_1 = 1.8$, $K_2 = 3.8$, $\psi = -1.016$ radians, and the experiment VLBI channel frequencies of 2.271 and 2.309 GHz. It can be seen in Fig. 8 that the two theoretical curves differ mainly in the amplitude damping features, as was explained in Section II of this article.

It can further be seen that for both theoretical curves and experimental data, the peak-to-peak values are approximately plus/minus 3 cm. Although peak-to-peak values are in reasonable agreement between theory and experiment, the periodicity is not in good agreement. This disagreement might partially be explained by the fact that the theoretical curve accounts only for the multipath signal produced by multiple bounces between the subreflector and flat surfaces behind the feedhorn. The experimental data include multipath errors over the entire antenna, including the quadripod supports.

V. Conclusions

The experiment to determine the effects of subreflector defocusing was successfully performed at an S-band frequency of 2290 MHz. It was determined that for the 64-m DSN antenna, axial subreflector defocusing results in a linear component of VLBI delay change equal to 1.8 times the axial defocus position. This information will be very useful for (1) correcting for unintentional subreflector movement due to gravity and/or (2) correcting for delay changes due to intentional or automatic refocusing which is sometimes purposely done to maximize antenna gain.

The observed peak-to-peak change of cyclical variation was about plus/minus 3 cm at 2290 MHz using a 38-MHz SBW. The cyclical variations are attributed to the multipath phenomenon. Although the measured delay changes due to multipath do not agree in detail with the relatively simple theoretical curves, the agreement achieved on error bounds between theory and experiment is a noteworthy achievement. The data presented in this article should be helpful in establishing worst-case error limits on VLBI measurements due to structural deformation of the antenna.

References

1. Katow, M. S., "DSS 14 64-m Antenna-Computed RF Pathlength Changes Under Gravity Loadings," *TDA Progress Report 42-64*, pp. 123-131, Jet Propulsion Laboratory, Pasadena, Calif., Aug. 15, 1981.

2. Otoshi, T. Y., and Rusch, W. V. T., "Multipath Effects on the Time Delays of Microwave Cassegrainian Antennas," *DSN Progress Report 42-50*, pp. 52-55, Jet Propulsion Laboratory, Pasadena, Calif., Apr. 15, 1979.

3. Otoshi, T. Y., "S/X Band Experiment: A Study of the Effects of Multipath on Group Delay," *Deep Space Network Progress Report 42-24*, pp. 40-50, Jet Propulsion Laboratory, Pasadena, Calif., Dec. 15, 1974. (See the Appendix entitled "Derivation of Equations for Phase and Group Delay Errors Caused by Multipath," Eqs. (A-11) and (A-12), p. 48.)

4. Thomas, J. B., "The Tone Generator and Phase Calibration in VLBI Measurements," in *The DSN Progress Report 42-44*, pp. 63-74, Jet Propulsion Laboratory, Pasadena, Calif., Apr. 15, 1978.

5. Levy, R., "VLBI Antenna Mechanical Calibration Work Unit," in *OSTDS Advanced Systems Review at JPL (DSN Advanced Systems Review)*, p. 92, June 24-26, 1980 (JPL/NASA document).

6. Freily, A. J., "Performance of DSS 13 26-m Antenna at X-Band, *"DSN Progress Report 42-30*, pp. 113-118, Jet Propulsion Laboratory, Pasadena, Calif., Dec. 15, 1975.

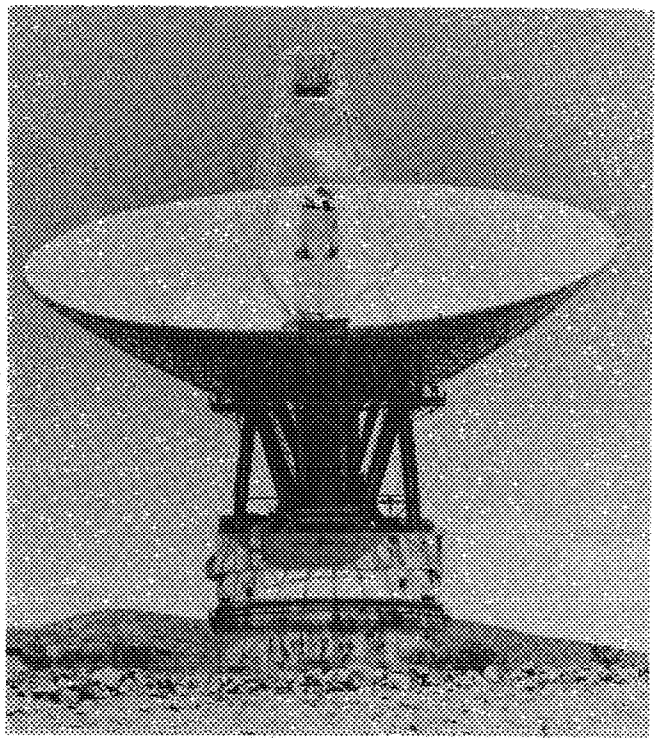

Fig. 1. DSN 64-m Cassegrain antenna at Goldstone, California

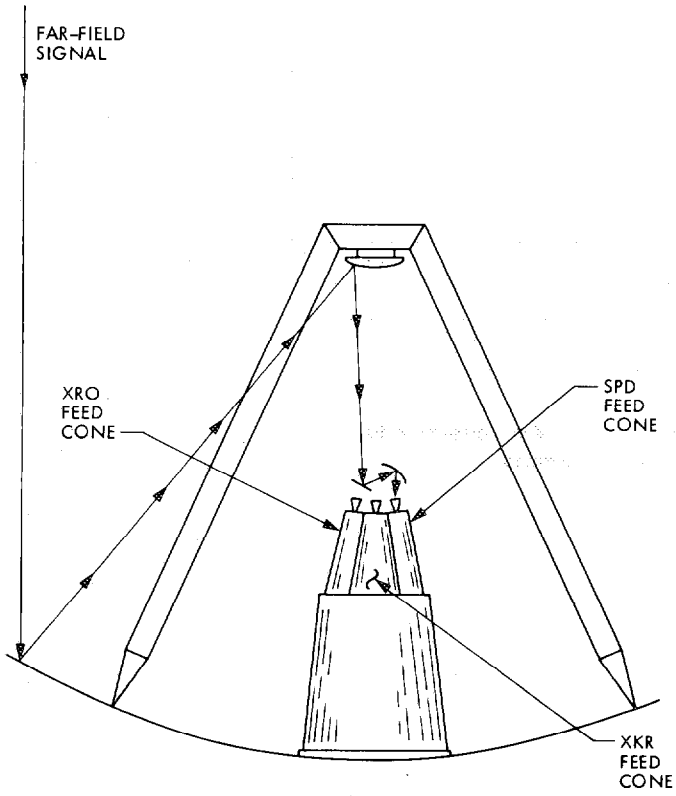

Fig. 2. Typical ray path for primary signal on DSN 64-m antenna

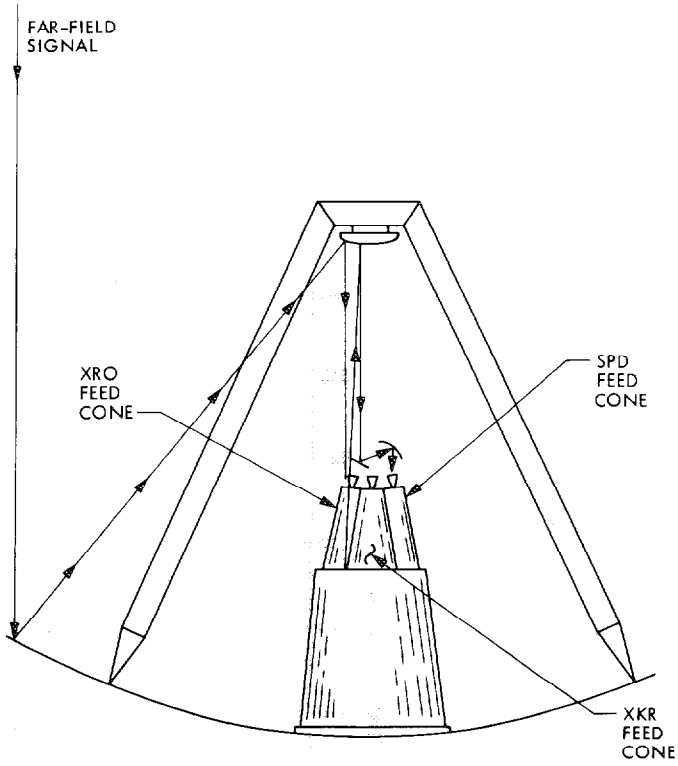

Fig. 3. A secondary propagation ray path on DSN 64-m antenna

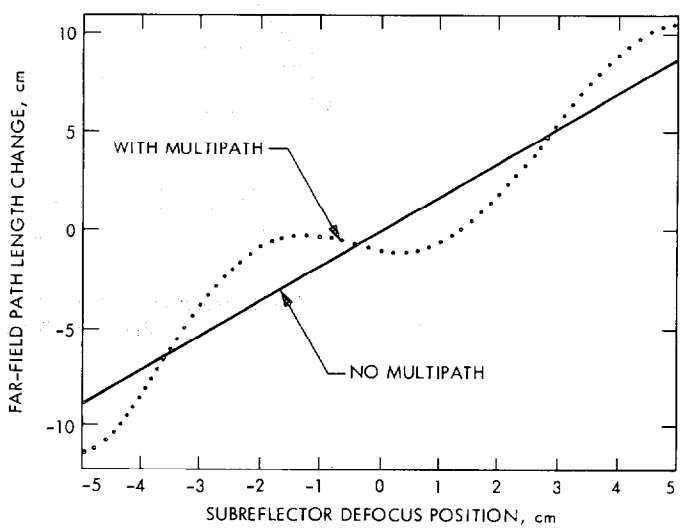

Fig. 4. Sample theoretical curve showing far-field delay changes due to subreflector defocusing on 64-m antenna at 2285-MHz and 40-MHz spanned bandwidth (from Ref. 2)

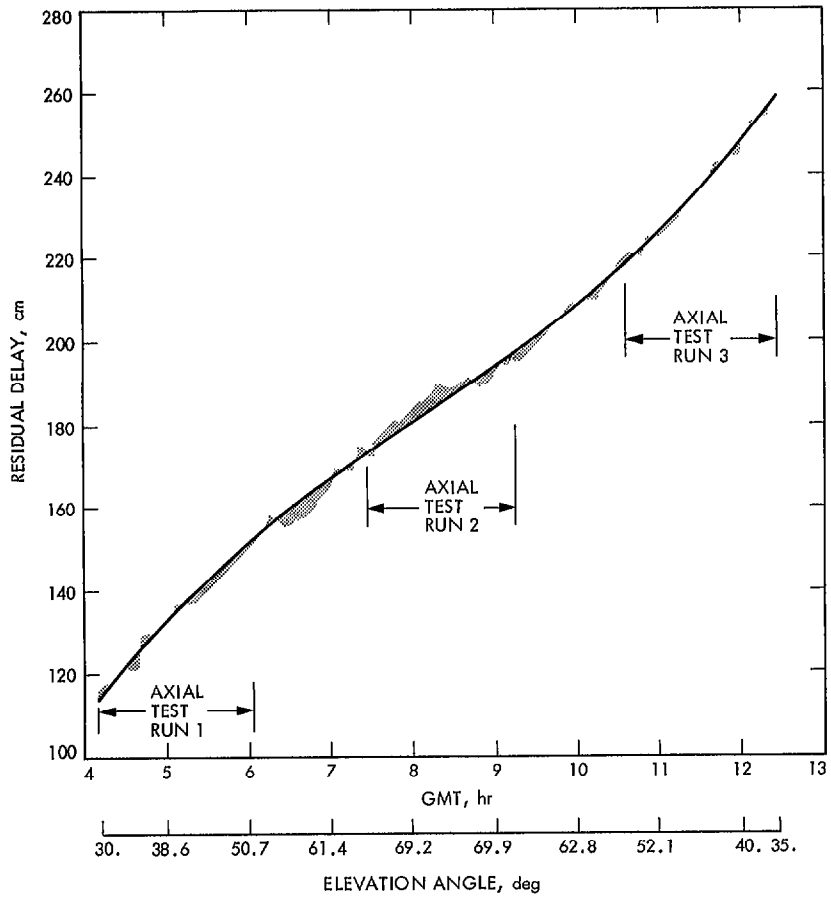

Fig. 5. Polynomial curve fit to nominal points after correlation to DSS 13-DSS 14 baseline is performed

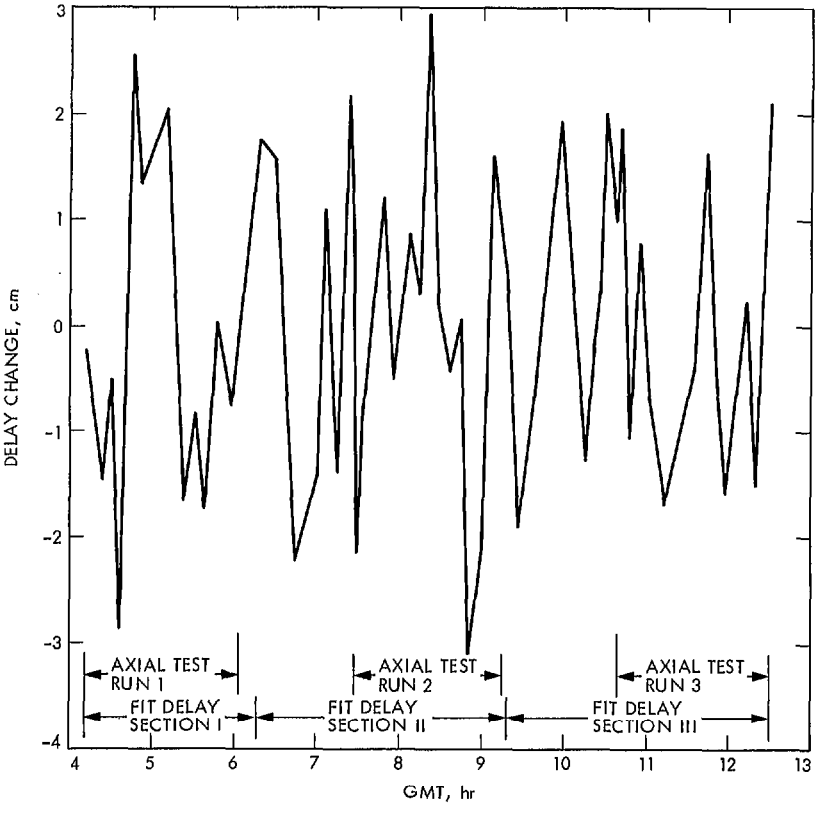

Fig. 6. Residuals of nominal points after residual clock errors and instrumental drift are removed

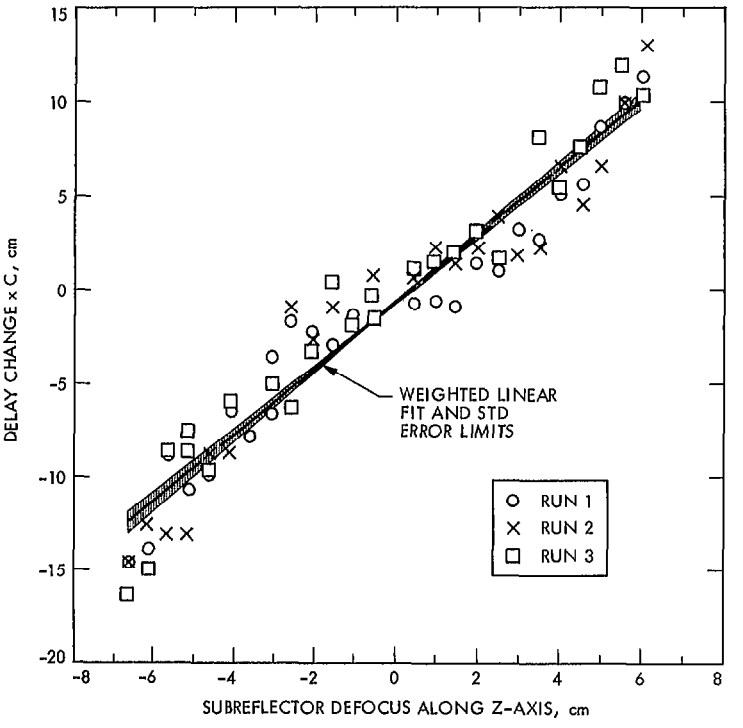

Fig. 7. Weighted least squares linear fit to processed VLBI data from axial subreflector tests on 64-m antenna at 2290 MHz

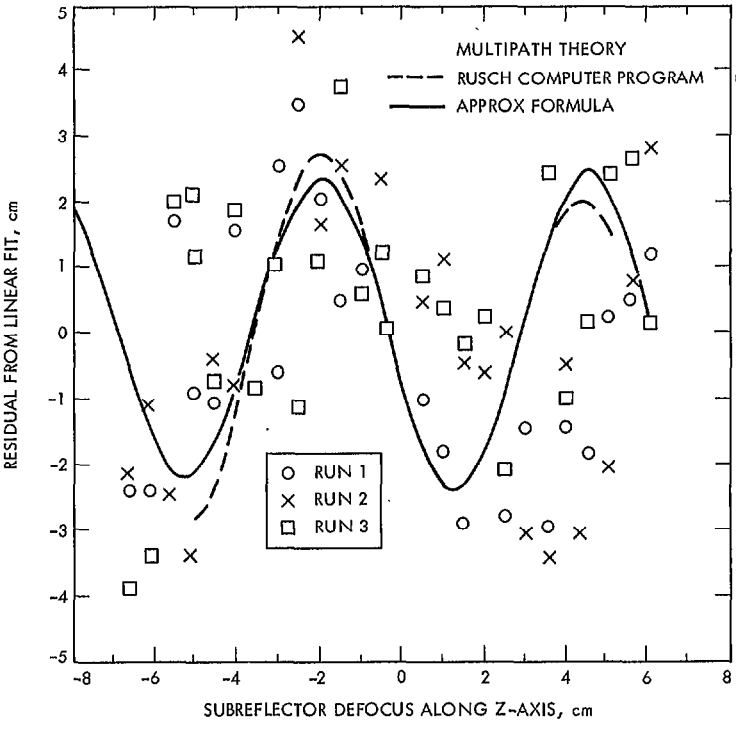

Fig. 8. Comparisons of multipath theoretical curves to experimental data which were derived by subtracting linear fit from VLBI data points (see Fig. 7)